Multifrequency High-Field EPR Study of Binuclear Mn(III)Mn(IV) Complexes[§]

Clotilde Policar,[†,1a] Moritz Knüpling,[1a,b] Yves-Michel Frapart,[‡,1c] and Sun Un*[,1a]

Département de Biologie Cellulaire et Moléculaire, Section de Bioénergétique, CNRS URA 2096, CEA Saclay, F-91191 Gif-sur-Yvette, France; Institut für Experimentalphysik, Freie Universität Berlin, D-14195 Berlin, Germany; Grenoble High Magnetic Field Laboratory, MPIF-CNRS, 25 avenue des Martyrs, BP 166, 38042 Grenoble Cedex 9, France; and Laboratoire de Chimie Inorganique, CNRS URA 420, Institut de Chimie Moléculaire d'Orsay, Université Paris XI, F-91405 Orsay Cedex, France

Received: May 4, 1998; In Final Form: July 13, 1998

The results from a multifrequency high-field EPR study of five di-μ-oxo bridged mixed-valence binuclear Mn(III)Mn(IV) complexes are reported. Spectra were obtained at 9, 95, and 285 GHz. The *g* anisotropy was unambiguously observable at 285 GHz. Hyperfine and **g** tensor values were estimated using spectral simulation procedures that cyclically and simultaneously fit the multifrequency data. In all five cases, the **g** tensors of the mixed-valence complexes were found to be rhombic. The **g** tensors were analyzed using the vector projection model. Most, but not all, of the *g* anisotropy originates from the Mn(III) center. The rhombic **g** tensors result from the low symmetry of the manganese centers. The size of the effective *g* anisotropy for a given complex was found to be a linear function of the average bond distance between the manganese and axial nitrogens. This relationship can be understood in terms of the influence of tetragonal distortion on the electronic levels of the Mn(III) center. The frequency-dependent line broadening observed in these mixed-valence complexes is explained in terms of the relationship between *g* anisotropy and structure.

The development of high-field electron paramagnetic resonance (HF-EPR) has made it possible to measure small *g* anisotropies (<0.01) which are difficult to resolve with conventional EPR without the use of single crystals. It has long been appreciated that *g* values of paramagnetic metal complexes can be related to their electronic structure.[2] Recently, studies of semiquinones and tyrosyl radicals indicate that even small *g* anisotropies of these radicals can be quantitatively related to the electronic structure of the radical and its electronic environment.[3,4] As the *g* anisotropy of radicals and many metal centers arises from a common spin−orbit coupling mechanism, a natural question is whether high-field EPR can be similarly utilized to study paramagnetic metals centers with intrinsically small *g* anisotropies. A class of metal complexes which have small *g* anisotropies are those with mixed-valence binuclear Mn(III)-Mn(IV) centers. All of the studies to date indicate that the *g* anisotropy is small ($\Delta g \leq 0.025$), but certainly larger than those of organic radicals and not resolvable at conventional magnetic fields.[5−8] Hence, these complexes provide an interesting challenge for high-field EPR.

Mixed-valence binuclear Mn(III)Mn(IV) centers play important biological roles.[9−12] In photosystem II, the catalytic site of water to oxygen conversion, the oxygen evolving center (OEC), is thought to be a four-manganese cluster.[10,13,14] The S_2 oxidation state of the OEC exhibits a well-resolved multiline EPR signal.[15] This signal has been assigned to a electronic spin-$^1/_2$ ground state, the large number of lines arising from hyperfine coupling of this effective spin-$^1/_2$ with four spin-$^5/_2$ manganese nuclei. Recently, a different multiline signal has been observed in the S_0 state.[16−19] Manganese catalase contains a dinuclear manganese active site. The catalytically inactive Mn(III)Mn-(IV) oxidation state of this protein exhibits a 16-line spectrum which also arises from a electronic spin-$^1/_2$ ground state.[20−23] Similarly, 16-line spectra are observed for synthetic binuclear mixed-valence di-μ-oxo Mn(III)Mn(IV) compounds.[5,10]

In this work, we present results from a high-field EPR study. We have used 95 GHz 3 T and 285 GHz 10 T as well as conventional 9 GHz 0.3 T EPR spectroscopies to study *g* values of model Mn(III)Mn(IV) complexes. As we will show, at 10 T, the *g* anisotropy is large enough to dominate the spectrum. To enhance our multiple-field approach, we studied five structurally and chemically related mixed-valence di-μ-oxo binuclear complexes all of which have known crystal structures: di-μ-oxobis{*N*,*N*′-bis(2-pyridylmethyl)-*N*,*N*′-dimethyl-1,2-ethanediamine}dimanganese(III,IV) perchlorate,[24] (referred to as bispicenMe); di-μ-oxobis{*N*,*N*′-dimethyl-*N*,*N*′-bis[(1-methylimidazol-2-yl)methyl]ethane-1,2-diamine}dimanganese(III,IV) perchlorate[25] (bisimMe); di-μ-oxobis{*N*,*N*′-dimethyl-*N*,*N*′-bis[(imidazol-4-yl)methyl]ethane-1,2-diamine}-dimanganese(III,IV) perchlorate[26](bisimH2); di-μ-oxotetrakis-(1,10-phenanthroline)dimanganese(III,IV) perchlorate[27] (phen); di-μ-oxotetrakis(2,2′-bipyridine)dimanganese(III,IV) perchlorate[28] (bipy). The structure of the ligands and a schematic representation of the complexes are shown in Figure 1. In each case, the manganese atoms are bonded to two bridging oxygens and four nitrogens from the ligands. Three of the ligands, bispicenMe bisimMe, and bisimH2, are tetradentate and possess two aromatic and two aliphatic nitrogens. The other two ligands, phen and bipy, are bidentate with two aromatic nitrogens. The general structure around the two manganese is pseudo-octahedral, with the two bridging oxygens and two manganese atoms defining the equatorial plane. The axial bond

[†] Current address: Laboratoire de Chimie Bio-organique et Bio-inorganique, CNRS URA 1384, Institut de Chimie Moléculaire d'Orsay, Université Paris XI, F-91405 Orsay Cedex, France.

[‡] Current address: Department of Biochemistry, Chemical Center Lund University, S22100 Lund, Sweden.

[§] This paper was originally submitted as part of the Klein/Sauer Festschrift [*J. Phys. Chem. B* **1998**, *102* (42)].

10.1021/jp982096d CCC: $15.00
Published on Web 11/18/1998

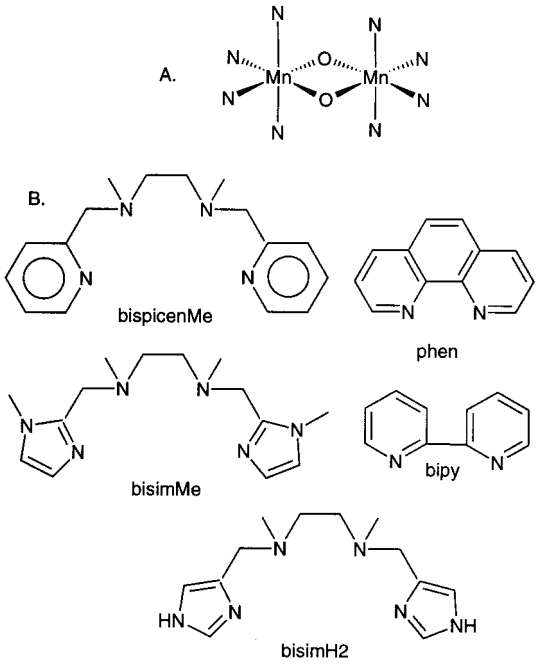

Figure 1. (A) A schematic structure of the di-μ-oxo bridged mixed-valence binuclear Mn(III)Mn(IV) complex and (B) the structure of the ligands.

lengths of Mn(III) of the bispicenMe, bisimH2, and bipy complexes are elongated, indicative of a Jahn−Teller effect. For the bisimMe and phen complexes, Mn(III) and Mn(IV) appear to be crystallographically equivalent (see below).[27] By using accurate *g*-value measurements made at high magnetic field and the known structures, we show that similar to organic radicals it is indeed possible to quantitatively analyze the variation in *g* anisotropy with structure of mixed-valence Mn(III)Mn(IV) complexes and that a mechanism for inhomogeneous line broadening in such systems can be deduced.

Theory

The electronic spin-$^1/_2$ ground state of the simple mixed-valence binuclear Mn(III)Mn(IV) center can be described by the effective spin Hamiltonian

$$H = \mathbf{S}\cdot\mathbf{G}\cdot\mathbf{H} + \mathbf{I}_1\cdot\mathbf{A}_1\cdot\mathbf{S} + \mathbf{I}_2\cdot\mathbf{A}_2\cdot\mathbf{S}$$

where $\mathbf{S}$, $\mathbf{I}_1$, and $\mathbf{I}_2$ are the vector spin operators and $\mathbf{G}$, $\mathbf{A}_1$, and $\mathbf{A}_2$ are the effective spin tensors. The characteristic 16-line spectrum of the model mixed-valence complexes results from the hyperfine coupling of the effective electronic spin-$^1/_2$ to two manganese nuclei when $|A_1| \approx 2|A_2|$, where A_1 and A_2 are the hyperfine coupling constants.[5] The relationship between the effective and the intrinsic spin tensors is given by the vector projection model:[29]

$$G = g^{\mathrm{III}}\frac{\mathbf{S}_1\mathbf{S}}{\mathbf{S}^2} + g^{\mathrm{IV}}\frac{\mathbf{S}_2\cdot\mathbf{S}}{\mathbf{S}^2} = 2g^{\mathrm{III}} - g^{\mathrm{IV}}$$

$$A_1 = a^{\mathrm{III}}\frac{\mathbf{S}_1\cdot\mathbf{S}}{\mathbf{S}^2} = 2a^{\mathrm{III}}$$

$$A_2 = a^{\mathrm{IV}}\frac{\mathbf{S}_2\cdot\mathbf{S}}{\mathbf{S}^2} = -a^{\mathrm{IV}} \qquad (2)$$

where g^{III} and g^{IV} are the intrinsic $\mathbf{g}$ tensors and a^{III} and a^{IV} the intrinsic hyperfine tensors of the Mn(III) ($S_1 = 2$) and Mn(IV) ($S_2 = {}^3/_2$) atoms, respectively.[30] The first-order expressions for the spin-orbit coupling contribution to the $\mathbf{g}$ tensors have been determined for both spin states using perturbation theory.

The ground-state term of a Mn(III)(d^4) center in an octahedral field is ^5E_g with a $^5T_{2g}$ excited-state. Under a tetragonal distortion, the ^5E_g state splits into a $^5A_{1g}$ and a $^5B_{1g}$ state with the ground-state determined by the nature of the distortion. The $^5T_{2g}$ state splits into a $^5B_{2g}$ and a ^5E_g state. The *g* values of the two possible ground states are given by[31,32]

$$g_{\parallel}^{\mathrm{III}} = g_{\mathrm{free}} - \frac{(4 \pm 4)\lambda}{\Delta}$$

$$g_{\perp}^{\mathrm{III}} = g_{\mathrm{free}} - \frac{(4 \mp 2)\lambda}{\Delta}$$

$$a_{\parallel}^{\mathrm{III}} = a_{\mathrm{iso}} \pm (2/7)\gamma\beta\beta_n\langle r^{-3}\rangle$$

$$a_{\perp}^{\mathrm{III}} = a_{\mathrm{iso}} \mp (1/7)\gamma\beta\beta_n\langle r^{-3}\rangle \qquad (3)$$

where the lower signs refer to the $^5A_1$ ground state and the upper, the $^5B_1$, Δ is the energy difference between the corresponding ground and excited states, and λ is the spin−orbit coupling constant. In the hyperfine equations, the two terms describe the isotropic and anisotropic components, respectively. Regardless of the Mn(III) ground state, $g_{\mathrm{iso}}^{\mathrm{III}}$ is given by $g_{\mathrm{free}} - 4\lambda/\Delta$ and $|\Delta g^{\mathrm{III}}|$ by $6\lambda/\Delta$.[30] The structure of the Mn(III) center in mixed-valence complexes (see below) is similar to Mn(III) in rutile (TiO_2) with the axial Mn−O(N) distance elongated relative the equatorial Mn−O(N) bond lengths. This distortion favors a $^5B_1$ ground state.[6,32] For this ground state, g_z^{III} (or $g_{\parallel}^{\mathrm{III}}$) will be directed along the axial (d_{z^2}) direction and have the lowest *g* value.[32] The hyperfine coupling is predicted to be the smallest along this direction.[32] The *g* values of a Mn(IV)(d^3) ion in a tetragonally or trigonally distorted octahedral field is given by[33]

$$g_{\parallel}^{\mathrm{IV}} = g_{\mathrm{free}} - (8\lambda/3\Delta_1)$$

$$g_{\perp}^{\mathrm{IV}} = g_{\mathrm{free}} - (8\lambda/3\Delta_2) \qquad (4)$$

where λ is the spin−orbit coupling constant, Δ_1 and Δ_2 are the energy differences between the $^4A_2$ singlet ground state and two sublevels of an orbital triplet $^4T_2$ excited state.[34] The hyperfine anisotropy for Mn(IV) ion is expected to be small in comparison to a Mn(III) ion.[31]

Values of the excitation energies and the spin−orbit coupling constant are required to estimate the manganese *g* values. In principle, the excitation energies can be obtained from optical spectra. The spin−orbit coupling constant for a manganese free ion is 85 cm^{-1} and can be as low as 60 cm^{-1} in some complexes due to effects of covalency.[32,33,35,36] The exchange coupling in Mn(III)Mn(IV) di-μ-oxo complexes is mediated by the partial covalent character of the Mn−O−Mn bonding.[37,38] Therefore, it is reasonable to assume that the spin−orbit coupling constant should be much lower than the free ion and a value 60 cm^{-1} is used in the analysis of the $\mathbf{g}$-tensor results present below. As will become apparent, this value yields reasonable consistency between the available optical data and $\mathbf{g}$-tensor measurements.

The electronic spin-$^1/_2$ ground state of the Mn(III)Mn(IV) complexes arises from an antiferromagnetic exchange coupling between the $S = 2$ and $S = {}^3/_2$ centers. The coupling in these complexes has been estimated to be about -300 cm^{-1}.[39] An excited state ($S = {}^3/_2$) of the system is about 450 cm^{-1} above the ground state. However, this low lying excited state will not contribute significantly to the $\mathbf{g}$ tensor. Implicit in both

eqs 4 and 3 is the fact that the ground and excited states must have identical spin multiplicities.[2] Interestingly, it can be shown that anisotropic spin−orbit coupling can induce anisotropy in the exchange interaction.[40]

Experimental Section

Complexes and Sample Preparations. The compounds were generous gifts of Dr. J.-J. Girerd and co-workers and prepared by usual synthetic procedures.[24−26] The EPR samples were prepared using recrystallized compounds and distilled anhydrous solvents and had an approximate concentration of 10^{-2} M and a volume of 100 μL. Spectra shown in this paper were obtained from samples prepared using a mixture of acetonitrile (MeCN) and *N*,*N*-dimethylformamide (DMF) at a ratio of 2:1. Experiments were also carried out with solvent mixtures containing alcohol and with acetonitrile containing 0.1 M tetraethylammonium perchlorate. Samples were frozen in liquid nitrogen immediately after preparation and kept frozen for the duration of the experiments. On freezing, the samples formed uniform glasses. The concentration dependence of the spectral resolution at 9 GHz was examined by comparing the spectra obtained at 10^{-3} and 10^{-2} M. No difference in the resolution was observed. As the signal-to-noise ratio was appreciably better at all the three frequencies for the 10^{-2} M samples we used these in the analysis. For the phen complex, up to 2.5 equiv of ligand was added without any effect to spectra taken at 95 and 285 GHz.

EPR Spectroscopy. All high-field data were obtained at the Grenoble High Magnetic Field Laboratory. A Gunn diode microwave source (Epsilon-Lambda, Geneva) capable of generating 100 mW of power over a 89−101 GHz frequency range was used as the fundamental microwave source. The frequency of the Gunn diode was stabilized by a source-locking counter (EIP, Santa Clara). Frequencies in the 284−296 GHz range were generated with a frequency tripler (Radiometric Physiks, Meckenheim) in conjunction with the Gunn oscillator. The microwave frequency used for a particular spectrum was determined by frequency stability and output power considerations which fluctuated from experiment to experiment. Hence, the spectra reported in this work were taken over a number of frequencies. The frequencies were accurate to 1 kHz. For simplicity, in the text, the spectra are referred to as 9, 95, and 285 GHz rather than the exact frequency. The microwave power was detected using a InSb bolometer (QMC, London). The other parts of the spectrometer have been previously described.[42] The limiting factor in the measurement of the *g* values was the accuracy of the magnetic field values. In the 10 T region, the absolute uncertainty in field measurement was estimated to be less than ± 0.001 in *g*, with a relative uncertainty of ± 0.0002. For the 3 T region, the calibration of the magnet was much poorer. The absolute errors were higher than at 10 T. However, the relative accuracy was the same. Because of the error in the absolute field measurement, the *g* values reported in this work have the greatest uncertainty in g_{iso},[30] while the deviations from g_{iso}, as given by $g_x - g_{iso}$, $g_y - g_{iso}$, and $g_z - g_{iso}$, reflect the high resolution obtainable at the high fields. High-field EPR data were obtained between 4.3 and 20 K under nonsaturating power conditions. Approximately 10 mW microwave power, as measured at the source, was used for the 95 GHz spectra and about 1 mW at 285 GHz. All 9 GHz spectra were recorded at 10 K on a Bruker ESP300.

Spectral Simulation. A perturbation equation including second-order terms in the hyperfine coupling was used to calculate the spectra.[43] The powder spectra were synthesized by calculating the resonant field for 3000−5000 random orientations[44] of the applied magnetic field with respect to the *g*-axes frame and summing the results assuming unit transition probability. The resulting orientation integrated spectrum was convolved with a derivative Gaussian line shape. The nine spin parameters were estimated by minimizing the root-means-square (rms) difference between the calculated and experimental spectra. Nonlinear minimization was achieved using standard simplex and conjugate gradient procedures.[45] The perturbation equation used for spectrum simulations are not sensitive to the sign of the hyperfine coupling constants. Collinear rhombic **g** and hyperfine tensors were assumed. As we will show for four of the five complexes studied, this simple collinear rhombic model yielded good fits and a more complicated model would appear to be unjustified. When the collinearity restriction was partially lifted, so that only one axis of **g** tensor was collinear with a hyperfine tensor axis, no improvement in the simulations was observed.

All calculations were performed on either a DEC Alphastation 250 (Maynard, MA) or a Gateway 2000 G5-200 using locally written programs based on the Fortran-77 subroutines found in the textbook by Press.[45] The subroutines were used with only modest nonsubstantive modifications.

Results

EPR Spectra. The 9 GHz spectra of the five mixed-valence manganese complexes exhibited the classical 16-line EPR signature and were identical to those previously published.[5,6,26] A typical 9 GHz spectrum is shown in Figure 4B. Small variations in apparent resolution and hyperfine splittings were observed between the five complexes. The overall extent of the spectra, as measured by the field separation between the first and last hyperfine line, was about 120 mT for the bisimMe, bispicenMe, and bisimH2 complexes and about 124 mT for the phen and bipy. The line width of the individual hyperfine resonances ranged from 0.20 to 0.30 mT. The 95 GHz spectra (Figure 2) were much more complex than the 9 GHz. The line width of the individual hyperfine features at 95 GHz varied with the molecule and ranged from 0.25 to 0.35 mT. The approximate overall extent of the 95 GHz spectra was about 150 mT, the precise value of which was molecule dependent. The six large sharp features in the bipy and phen spectra are due to Mn(II).[46] The 285 GHz spectra (Figure 3) varied greatly from molecule to molecule. Sharp resonances arising from Mn(II) ions were observed for the bisimMe, phen, and bipy complexes. The overall spectral extent of a 285 GHz spectrum was difficult to specify, as the hyperfine intensities were weak especially on the high-field portion of the spectra. For the phen spectrum, where the first and last hyperfine features are well-defined (Figure 2D), the extent was approximately 210 mT. The increase in the extent of the 285 GHz spectra compared those obtained at 9 and 95 GHz is a clear indication of *g* anisotropy. If one assumes that the extent of the 9 GHz spectra is largely determined by hyperfine interactions, then an estimate of the *g* anisotropy is 10^{-2} (i.e., (210−120 mT)/10 T). Estimates of the *g* anisotropy obtained directly from 285 GHz data in this manner are summarized in Table 1. The width of the individual hyperfine features at 285 GHz were larger than at the two lower frequencies, with a minimum value of 0.50 mT. All complexes exhibited lower hyperfine resolution along the high-field edge of the spectra in comparison to the low-field edge, clearly demonstrating the presence of hyperfine anisotropy. This is most clearly seen in bisimMe spectrum (Figure 3A). The hyperfine splittings were similar in the middle and low-field

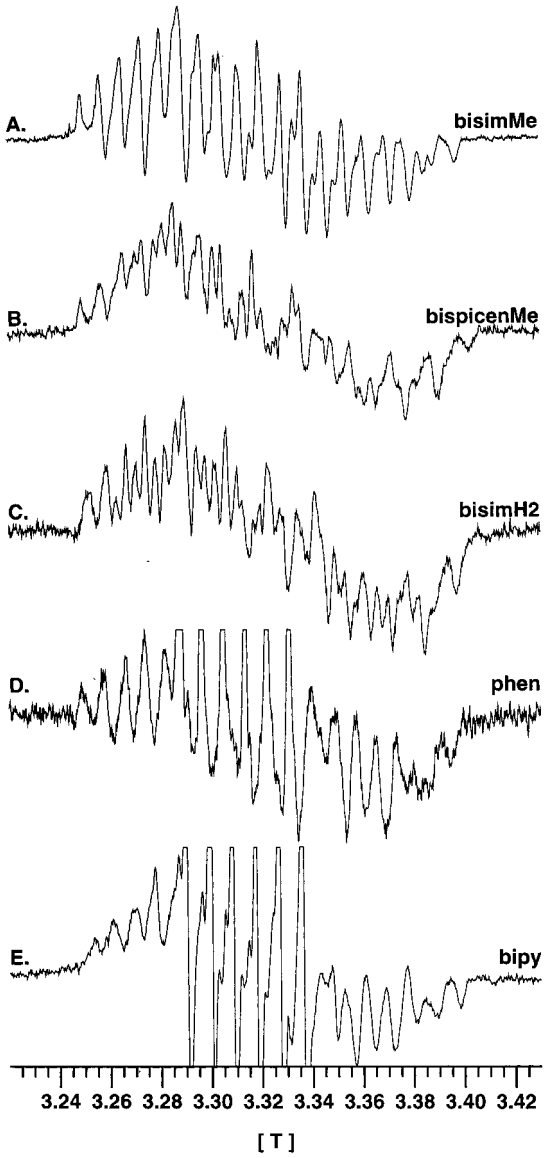

Figure 2. The 95 GHz 3 T spectra of the five mixed-valence Mn(III)Mn(IV) complexes. The field axis of each spectra has been manually adjusted to align the lowest field features to facilitate comparisons. Spectra D and E have been vertically truncated. The six central lines in these two spectrum arise from Mn(II). All spectra were obtained in a DMF/MeCN (1:2) solvent mixture at 10 K with 7−8 G modulation amplitude and 100 kHz modulation frequency under nonsaturating conditions. (see text and Figure 1 for abbreviations).

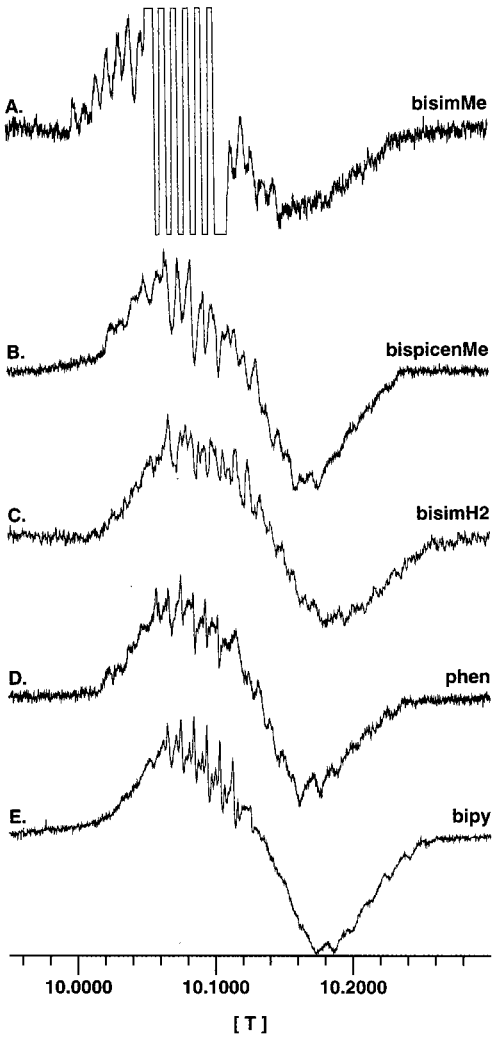

Figure 3. The 285 GHz 10 T EPR spectra of the five mixed-valence Mn(III)Mn(IV) complexes in DMF/MeCN (1:2). To facilitate comparisons between spectra, the field axis has been scaled using the formula $Hf_{obs}/282.640$, where f_{obs} is the microwave frequency and H is the magnetic field. Spectrum A (bisimMe) was obtained with a microwave frequency of 282.640 GHz. All spectra were obtained between 4.2 and 20 K with 7−8 G modulation amplitude and 100 kHz modulation frequency under nonsaturating conditions. The six truncated lines of spectrum A are due to Mn(II).

regions of the spectrum. These observations are consistent with eq 3 and with a recent study based on ENDOR spectroscopy and 9 and 35 GHz EPR.[7]

For all five complexes studied, the spectral resolution was highly dependent on the nature of the solvent. In general, poor spectral resolution at 9 GHz was indicative of poor resolution at higher frequencies. However, samples with good resolution at 9 GHz did not necessarily have good resolution at high frequencies. A variety of solvents and mixed solvents were tested. The solvent composition used in this work, a 2:1 mixture of acetonitrile and DMF, gave the best resolution and the smallest Mn(II) signals. Alcohol-containing solvent mixtures yielded comparable resolution to that of the acetonitrile−DMF mixture, but always resulted in much bigger Mn(II) signals.[46]

Estimation of Spin Parameters. In order to estimate quantitatively the spin tensors, we simulated the experimental spectra. The rms difference between the calculated and experimental spectra is determined by the three g values, nine hyperfine tensor elements, and one normalization constant and is likely to have a large number of local minima.[45] Therefore, in order to obtain the global minimum, a procedure was developed that involved a cycle of three sequential minimizations of just the 9 and 285 GHz data based on a simplex algorithm.[45] First, the 285 GHz spectrum was minimized using 500 randomly chosen starting parameters. The parameters obtained were refined by a simulation of 9 GHz data. A final refinement of the spin parameters was obtained by a resimulation of the 285 GHz spectrum. This minimization procedure was undertaken because the 285 GHz data although poorly resolved with respect to hyperfine couplings had resolved g anisotropy while the opposite situation held for the 9 GHz spectra.[47] The standard deviation of the 50 best fits was 5×10^{-4} in g (which corresponds to 25 G at 285 GHz) and 5 MHz for the hyperfine couplings. The spin parameters obtained by the cyclic procedure were tested by simultaneous fittings of 9, 95, and 285 GHz using a conjugate gradient technique. This second method was developed not to be exhaustive, but rather to be a simple method

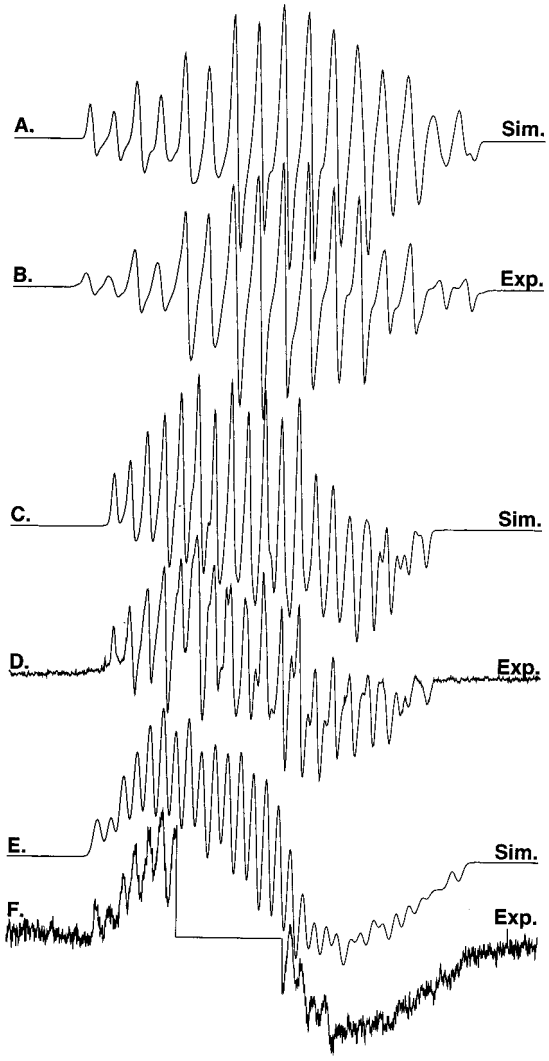

Figure 4. Simulations of the bisimMe spectra obtained by a simultaneous fit of the 9 (A, B), 95 (C, D), and 285 GHz (E, F) experimental spectra (see text for details). The 95 GHz spectrum was obtained at 4.2 K and 285 GHz at 20 K. For 285 GHz simulation, the Mn(II) region of the spectrum has been considered in the minimization.

TABLE 1: Estimates of the Effective *G* Anisotropy Based on the Extent of the 9 and 285 GHz Spectra

compound	ΔG	compound	ΔG
bisimMe	0.022	bipy	0.019
bispicenMe	0.018	phen	0.017
bisimH2	0.021		

for checking consistency between the estimated parameters and the data obtained at 95 GHz. Depending on the intensity of the Mn(II) resonances, regions of the 285 and 95 GHz spectra containing these signals were excluded from both minimization calculations (Figure 4). The final values obtained by the two methods are summarized in Table 2.

Of the five complexes studied, we were able to obtain reliable *g* and hyperfine tensor estimates for four of the complexes: the bisimH2, bisimMe, bipy, and phen. These are typified by the simulations of the bisimMe spectra shown in Figure 4. Apparently, the exclusion of the middle portion of the 285 GHz bisimMe spectra due to large Mn(II) resonance did not significantly affect the fitting procedures. The spin parameters for the bipy complex from our multifrequency study are in agreement with earlier analysis based on the 9 GHz spectrum and completely anisotropic spin tensors.[6] The poorest fits were

TABLE 2: Effective Spin Parameter Values Determined from Simulation of 9, 95 and 285 GHz EPR Spectra[a]

compound	G_{iso}	$G_x - G_{iso}$	$G_y - G_{iso}$	$G_z - G_{iso}$	ΔG
bisimMe	1.9927	0.0095	0.0036	−0.0131	0.0226
bispicenMe	1.9968	0.0087	0.0002	−0.0090	0.0177
bisimH2	1.9920	0.0100	0.0015	−0.0114	0.0214
bipy	1.9917	0.0088	0.0025	−0.0112	0.0200
bipy[b]	1.991	0.007	0.001	−0.009	0.0160
phen	1.9922	0.0080	0.0028	−0.0108	0.0188

compound	$\lvert A_{1x}\rvert$	$\lvert A_{1y}\rvert$	$\lvert A_{1z}\rvert$	$\lvert A_{2x}\rvert$	$\lvert A_{2y}\rvert$	$\lvert A_{2z}\rvert$
bisimMe	445	475	337	224	210	230
bispicenMe	456	460	351	217	213	223
bisimH2	464	464	362	219	217	223
bipy	502	472	345	214	207	229
bipy[b]	498	483	378	211	214	231
phen	495	468	339	211	211	233

[a] Hyperfine couplings are MHz. The uncertainty in G_{iso} is 0.001, in $G_i - G_{iso}$ 5 × 10^{-4} and in A 5 MHz (see text for details). [b] Zheng et al.[6]

obtained for the bispicenMe complex. Reasonable simulations of the 9 and 285 GHz data of bispicenMe complex using the sequential technique were obtained. However, we were unable to achieve a simultaneous fit of the three frequency data which was of the same quality as for the other complexes. Although the simulations for the bispicenMe complex are poor in the detail, the *g* anisotropy obtained for the simulations is exactly equal to estimates shown in Table 1 and the hyperfine values were entirely consistent with the other complexes. The only parameter which differed from the others was the isotropic *g* value. As this parameter carried the largest experimental error (see above), we were unable to determine how meaningful this difference was. Finally, we note that in all five cases, the effective *g* anisotropy, ΔG, obtained from the simulations (Table 2) are in good agreement with estimates directly obtained from the 9 and 285 GHz data summarized in Table 1.

An important benefit of HF-EPR in the study of the mixed-valence complexes was apparent. For a single spectrum taken at a given frequency, it was always possible to obtain a simulation which was statistically a better fit of the experiment than when either of the two multifrequency strategies were followed. In fact, it was possible to obtain spin parameters which yielded good simulations of the 9 GHz data that did not correctly predict the higher frequency spectra. This was not completely unexpected. Previously reported 9 GHz simulations were found to be in good agreement with the experiment data in spite of the fact that axial **g** tensors were assumed.[5,26] In some cases, it has been observed that rhombic tensors yield better simulations than axial ones.[7,6,48,49] Axial **g** tensors are clearly inconsistent with the 285 GHz data. Our study indicates that *g* anisotropies obtained from simulations of conventional 9 GHz data are not completely reliable. Furthermore, as the *g* anisotropy contribution is about 100 MHz (30 G) at 9 GHz, errors in estimation of *g* anisotropy are likely to influence estimations of the hyperfine tensor. These observations illustrate the importance of multifrequency high-field data where the *g* anisotropy can be resolved.

In the simulations, the hyperfine tensors were assumed to be collinear with **g** tensor. However, because of the relatively high resolution in *g* obtainable with large applied magnetic fields, this assumption was not particularly restrictive in the determination of the *g* values. The maximum error associated with this assumption is the size of the anisotropic portions of the hyperfine tensor. A more conservative upper-bound estimate of the error is 500 MHz, the size of the largest hyperfine

couplings. At 10 T, this error amounts to an uncertainty of only 0.001 in g (180 G). Therefore, the estimates of the g values at this level of accuracy are independent of the collinearity assumption. For the four complexes for which we obtained good simulations, the accuracy in the g values should be much higher than 0.001. As will be shown, even at the level of 0.001 uncertainty in g, it was possible to correlate the structure of these mixed-valence complexes to their g values.

Discussion

The results of the simulations can be analyzed in terms of vector projection equations (eq 2) and g value expressions for the isolated Mn(III) and Mn(IV) centers (eqs 4 and 3). **g** tensors have been measured for Mn(IV) ions in α-Al_2O_3[50] and MgO.[33] For the latter, $g_{||}^{IV}$ was found to be 1.9931 and $g_{\perp}^{IV}$ 1.9940. Application of eq 4 using optical data yields completely consistent results. For Mn(III)Mn(IV) complexes, bands at 18 000 and 23 000 cm^{-1} have been assigned to the Mn(IV) $^4A_2 \leftrightarrow {}^4T_2$ transitions.[37] Substituting these values into eq 4 gives a $g_{||}^{IV}$ value of 1.993 and a $g_{\perp}^{IV}$ value of 1.995, yielding a g_{iso}^{IV} of 1.995 and Δg^{IV} of 0.002. Although small, this anisotropy amounts to 360 G using an applied field of 10 T. Recently, HF-EPR measurements have been carried out on Mn(III) ions in a tetragonally distorted environment.[51] The estimated $g_{||}^{III}$ was 1.97 and $g_{\perp}^{III}$ 1.99, leading to a g_{iso}^{III} value of 1.99 and Δg^{III} of 0.02. If these values are assumed to be appropriate for the mixed-valence complexes, the Mn(III) contribution to ΔG is expected to be 0.04. A smaller estimate of the Mn(III) contribution is obtained by estimating g_{iso}^{III} using g_{iso}^{IV} in conjunction with the G_{iso} values obtained from our experiments.[52] Excluding the bispicenMe complex, the average G_{iso} for the complexes is about 1.992 (Table 2). When this value and the estimated g_{iso}^{IV} are substituted into eq 2, a g_{iso}^{III} value of 1.993 is obtained. This isotropic value implies that $|\Delta g^{III}|$ is 0.013 (eq 3, a Mn(III) contribution of 0.026 to ΔG). Taken together, a ΔG value of 0.024 is obtained. This ΔG estimate is slightly higher than the measured values, 0.022−0.018 for the five complexes, but given the approximations, agreement appears to be quite good. Most of the g anisotropy of the mixed-valence complexes clearly arises from the Mn(III) center. The Mn(IV) ion in the complexes contributes 10−20% to the total g anisotropy. The effect of the zero-field and exchange interactions on the effective g values was neglected in eq 2. This contribution[6] is given by

$$(2/5)(g_{III} - g_{IV})(7D_{III} + 2D_{IV})/J \qquad (5)$$

D_{III} is estimated to be about 4 cm^{-1}, D_{IV} 0 cm^{-1}, and J 300 cm^{-1}.[6,32,33,50] The value of $g_{III} - g_{IV}$ cannot exceed ΔG ($\sim$0.02). These values lead to an upper bound for the zero field and exchange contribution of 7×10^{-4} in g, a relatively small contribution which is on the order of the uncertainty in the g values obtained from the simulations. Except for the need to use reduced spin−orbit coupling values, the above analysis also indicates that, consistent with theory given in the previous section, the exchange coupling does not in any obvious manner contribute to the g anisotropies of the mixed-valence complexes.

In the preceding discussion, we have ignored the fact the effective **g** tensors are rhombic for all of the complexes. Equations 3 and 4 imply that the effective **g** tensor is axial. This discrepancy arises from the fact that the symmetries of the manganese centers are lower than those assumed by eqs 3 and 4. The two observed Mn(IV) $^4A_2 \leftrightarrow {}^4T_2$ optical transitions result from the nondegeneracy of the d_{xz} and d_{yz} orbitals where the former is of higher energy due to the bonding interactions with bridging oxygen p-orbitals.[37] It is reasonable that the d_{xz} and d_{yz} orbitals centered on the Mn(III) are also nondegenerate for the same reason. With this reduction in symmetry, the energy difference between the ground and excited states will be different in each of the three canonical directions, as well as the degree of spin−orbit mixing leading to a rhombic **g** tensor.

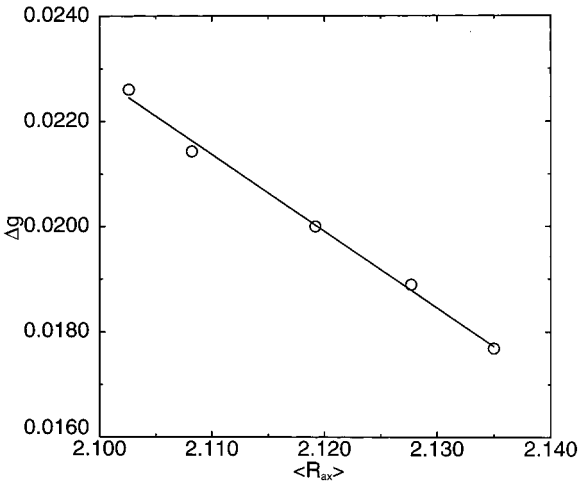

Figure 5. Effective G anisotropy ($G_x - G_z$) as a function of the average of the four Mn−nitrogen axial distances ($\langle R_{ax} \rangle$). $\langle R_{ax} \rangle$ values were calculated from the crystal structures (see text for details).

The energy difference, Δ, between the ground and excited states should be dominated by the first coordination sphere. Therefore, it is reasonable to assume that **g** tensors should be related to the structure of the mixed-valence manganese complexes. Unfortunately, two of the five crystallographic structures do not resolve the Mn(III) and Mn(IV) centers and they represent the average about these two centers.[27] This problem was compounded by a relative large uncertainty in g_{iso} (see above). To partially overcome these problems, we examined the behavior of ΔG as a function of the average of all four axial Mn−N distances (Figure 5). A striking linear trend was found. No trends were found when the equatorial nitrogens were averaged with the axial nitrogens or considered separately. If the small anisotropic contribution of Mn(IV) center is neglected, ΔG is simply twice Δg^{III} or $12\lambda/\Delta$ (eq 3). Hence, ΔG is expected to be linearly proportional to Δ^{-1}. For a d^4 ion, the ground-state splitting of the octahedral $^5E_{2g}$ level, due to elongation along the axial (or z) direction, is expected to be large since the $(t_{2g})^3(e_g)^1$ electron configuration involves a σ antibonding electron.[34] The splitting of the excited state is expected to be much smaller.[34] As Δ is determined by the energy difference between the $^5B_1$ ground state and $^5B_2$ excited state, it is expected that Δ will be sensitive to the extent of axial distortion and, therefore, the axial Mn−N bond distance.

The preceding discussion suggests a model for the frequency-dependent broadening or g strain that was described in the previous section. Under the most favorable conditions, the line widths of the resolved hyperfine features at 9 and 95 GHz were approximately the same and the 285 GHz line widths were at least twice as large. However, there were numerous solvents and solvent combinations which yielded good resolution at only 9 GHz, but which resulted in no hyperfine resolution at higher frequencies. This suggests that the broadening is not due to magnetic dipolar interactions that would occur with microcrystal formation in the glass. Such interactions are not field dependent. The likely explanation is that the solvents induce structural heterogeneity which in turn causes a distribution in the g values.

From Figure 5, it is clear that small distribution in axial Mn−N distances will lead to appreciable broadening. A change in distance of 0.001 Å will lead to a change in g anisotropy of 0.0001 or about 0.5 mT at 285 GHz. In principle, this form of solvent-induced line broadening should be also anisotropic. However, the simultaneous presence of hyperfine anisotropy makes this additional anisotropy difficult to detect.

Conclusion

With multifrequency high-field EPR, it is possible to obtain reliable estimates of the small g anisotropies of di-μ-oxo-bridged mixed-valence binuclear Mn(III)Mn(IV) complexes. The intrinsic **g** and hyperfine tensors of the Mn(III) and Mn(IV) centers have been deduced using the vector projection technique and equations for **g** tensors available from the literature. The **g** tensors for both manganese centers are anisotropic and in the case of Mn(III), completely rhombic. This results from the low electronic symmetry of the metal centers. Empirical structural correlations to the **g** tensors also provided insights into the mechanism of g strain. The value of the **g** tensors were found to be entirely consistent with electronic properties of the Mn(III) and Mn(IV) determined from optical spectroscopic measurements and hold the promise of using **g** tensors as another means of probing the electronic structure of the mixed-valence manganese centers, as well as the isolated Mn(III) and Mn(IV) centers. These conclusions show that HF-EPR can be used as an effective tool to probe the electronic structure of paramagnetic metal centers with intrinsically small g anisotropies.

Acknowledgment. This research was supported by a grant from the Human Frontiers Science Organization (contract No. RGO349) and by the E.U. through HCM grant ERBCHRX-CT940524. M.K. and C.P. acknowledge the CEA for fellowships. We thank Jean-Jacques Girerd and co-workers for their generous gift of the complexes and helpful comments. A. W. Rutherford is acknowledged for helpful discussions and encouragement.

References and Notes

(1) (a) CEA Saclay. (b) FU-Berlin. (c) Université Paris XI.

(2) Griffith, J. S. *The theory of transition-metal ions*; Cambridge Press: Cambridge, UK, 1961.

(3) Un, S.; Atta, M.; Fontecave, M.; Rutherford, A. W. *J. Am. Chem. Soc.* **1995**, *117*, 10713−10719.

(4) Knüpling, M.; Törring, J. T.; Un, S. *Chem. Phys.* **1997**, *219*, 291−304.

(5) Cooper, S. R.; Dismukes, G. C.; Klein, M. P.; Calvin, M. *J. Am. Chem. Soc.* **1978**, *100*, 7248−7252.

(6) Zheng, M.; Khangulov, S. V.; Dismukes, G. C.; Barynin, V. V. *Inorg. Chem.* **1994**, *33*, 382−387.

(7) Zwyegart, W.; Bittl, R.; Wieghardt, K.; Lubitz, W. *Chem. Phys. Lett.* **1996**, *261*, 272−276.

(8) Horner, O.; Charlot, M. F.; Boussac, A.; Anxolabéhère-Mallart, E.; Tchertanov, L.; Guilhem, L.; Girerd, J. J. *Eur. J. Inorg. Chem.*, in press.

(9) Dismukes, G. C. *Chem. Rev.* **1996**, *96*, 2909−2926.

(10) Larson, E. J.; Pecoraro, V. L. In *Introduction to manganese enzymes*; Pecoraro, V. L., Ed.. VCH Publishers: New York, 1992; pp 1−28.

(11) Wieghardt, K. *Angew. Chem., Int. Ed. Engl.* **1989**, *28*, 1153−1172.

(12) Dismukes, G. C. In *Bioinorganic Catalysis*; Reedijk, J., Ed.; VCH Publishers: New York, 1993; pp 317−346.

(13) Yachandra, V. E.; Sauer, K.; Klein, M. *Chem. Rev.* **1996**, *96*, 2927−2950.

(14) Rüttinger, W.; Dismukes, G. C. *Chem. Rev.* **1997**, *97*, 1−24.

(15) Dismukes, G. C.; Siderer, Y. *Proc. Natl. Acad. Sci. U.S.A.* **1981**, *78*, 274−278.

(16) Messinger, J.; Nuggent, J. H. A.; Evans, M. C. *J. Am. Chem. Soc.* **1997**, *36*, 11055−11060.

(17) Ahrling, K. A.; Petersin, S.; Styring, S. *Biochemistry* **1997**, *36*, 13148−13152.

(18) Messinger, J.; Robblee, J. H.; Yu, W. O.; Sauer, K.; Yachandra, V. K.; Klein, M. P. *J. Am. Chem. Soc.* **1997**, *119*, 11349−11350.

(19) Campbell, K. A.; Peloquin, J. M.; Pham, D. P.; Debus, R. J.; Britt, R. D. *J. Am. Chem. Soc.* **1998**, *120*, 447−448.

(20) Khangulov, S. V.; Barynin, V. V.; Antonyuk-Barynina, S. V. *Biochim. Biophys. Acta* **1990**, *1020*, 25−33.

(21) Khangulov, S. V.; Barynin, V. V.; Voevodskaya, N. V.; Grebenko, A. I. *Biochim. Biophys. Acta* **1990**, *1020*, 305−310.

(22) Fronko, R. M.; Penner-Hahn, J. E.; Bender, C. J. *J. Am. Chem. Soc.* **1988**, *110*, 7554−7555.

(23) Haddy, A.; Waldo, G. S.; Sands, R. H.; Penner-Hahn, J. E. *Inorg. Chem.* **1994**, *33*, 2677−2682.

(24) Glerup, J.; Goodson, P. A.; Hazell, A.; Hazell, R.; Hogdson, D. J.; McKenzie, C. J.; Michelsen, K.; Rychelwska, U.; Toflund, H. *Inorg. Chem.* **1994**, *33*, 4105−4111.

(25) Frapart, Y.-M.; Girerd, J.-J., unpublished results.

(26) Frapart, Y.-M.; Boussac, A.; Albach, R.; Anxolabéhère-Mallart, E.; Delroisse, M.; Verlhac, J.-B.; Blondin, G.; Girerd, J.-J.; Guilhem, J.; Cesario, M.; Rutherford, A. W.; Lexa, D. *J. Am. Chem. Soc.* **1996**, *118*, 2669−2678.

(27) Stebler, M.; Ludi, A.; Bürgi, H.-B. *Inorg. Chem.* **1986**, *25*, 4743−4750.

(28) Plaskin, P. M.; Stoufer, R. C.; Mathew, M.; Palenik, G. J. *J. Am. Chem. Soc.* **1972**, *94*, 2121−2122.

(29) Sands, R. H.; Dunham, W. R. *Q. Rev. Biophys.* **1975**, *7*, 443−504.

(30) Upper case letters denote effective spin parameters, lower case letters denote intrinsic parameters, and superscripts denote oxidation state. The convention $g_x \geq g_y \geq g_z$ is used and direction subscripts do not necessarily denote directions in the molecular frame. The quantity Δg, the anisotropy in g, is defined by $g_x - g_z$ and g_{iso} is defined as $1/3(g_x + g_y + g_z)$.

(31) Abragam, A.; Pryce, M. H. L. *Proc. R. Soc.* **1951**, *205*, 135−153.

(32) Gerritsen, H. J.; Sabisky, E. S. *Phys. Rev.* **1963**, *132*, 1507−1512.

(33) Davies, J. J.; Smith, S. R. P.; Wertz, J. E. *Phys. Rev.* **1969**, *178*, 608−612.

(34) Lever, A. B. P. *Inorganic Electronic Spectroscopy*; Elsevier: Amsterdam, 1984.

(35) Jorgensen, C. K. *Discuss. Faraday Soc.* **1958**, *26*, 110−115.

(36) Caneschi, A.; Gatteschi, D.; Sessoli, R. *J. Chem. Soc., Dalton Trans.*, in press.

(37) Gamelin, D. R.; Kirk, M. L.; Stemmler, T. L.; Pal, S.; Armstrong, W. H.; Penner-Hahn, J. E.; Solomon, E. I. *J. Am. Chem. Soc.* **1994**, *116*, 2392−2399.

(38) Anderson, P. W. In *Magnetism*; Rado, G. T., Suhl, H., Eds.; Academic Press: New York, 1963; pp 317−346.

(39) The exchange interaction is defined as $-J\mathbf{S}_1\cdot\mathbf{S}_2$.

(40) Bencini, A.; Gatteschi, D. *Electron paramagnetic resonance of exchange coupled systems*; Springer-Verlag: New York, 1990.

(41) Cooper, S. R.; Calvin, M. *J. Am. Chem. Soc.* **1977**, *99*, 6623−6630.

(42) Muller, F.; Hopkins, M. A.; Coron, N.; Grynberg, M.; Brunel, L.-C.; Martinez, G. *Rev. Sci. Instrum.* **1989**, *60*, 3681−3684.

(43) Taylor, P. C.; Baugher, J. F.; Kriz, H. M. *Chem. Rev.* **1975**, *75*, 203−240.

(44) Marsaglia, G. *Ann. Math. Stat.* **1972**, *43*, 645−646.

(45) Press, W. H.; Flannery, B. P.; Tenkolski, S. A.; Vetterling, W. T. *Numerical receipes (FORTRAN version)*; Cambridge University Press: Cambridge, UK, 1989.

(46) The Mn(II, $S = {}^5/_2$) lines that are sharp and clearly identifiable at 285 GHz are not observed at 9 GHz. This is directly related to the nonnegligible zero-field splitting of the Mn(II) ions. It has been shown that the line width of the individual hyperfine resonances is dependent on the ratio of the zero-field splittings to the applied magnetic field.[53] At 9 GHz, the zero-field coupling is sufficiently large compared to the Zeeman interaction to render the Mn(II) unobservable and, at 285 GHz, the opposite is likely to be true and the line width is determined by unresolved hyperfine couplings rather than the zero-field coupling. As only Mn(II) signals that arise from the $m_s = -{}^1/_2 \leftrightarrow m_s = {}^1/_2$ electron spin transition are observed, the observed intensity does not obey Curie behavior because the $m_s = -{}^1/_2$ level is not the ground state. Hence, one effective means of suppressing the Mn(II) signals is to reduce the observation temperature. This has the added advantage that the resonances arising from the mixed valence complexes become more intense with decreasing temperature since these signals arise from the ground state. The only disadvantage of using lower temperatures is the increased potential for saturation and passage artifacts. The spectra shown in Figures 2 and 3 were free of such artifacts.

(47) The fitting procedure started with the generation of 500 random starting points. These initial points were centered about the approximate g value corresponding to the center of the spectrum and 210 and 410 MHz for the two hyperfine couplings. The random starting points were distributed over a range of ±0.03 for G and ± 50 MHz for both hyperfine couplings. The resulting 500 minimized sets were sorted according to the RMS residual and the 50 best were retained and analyzed. In all cases, these 50 represented a single consistent set of the nine spin parameters. The spin parameters were further refined by a separate fitting of the 9 GHz data. Five hundred

random starting points were generated centered about the mean value of the set of 50 best parameters. To ensure consistency between the 9 and 285 GHz data, a final round of minimization was carried out on the 285 GHz data using the 9 GHz refined estimates. For the high-field spectra, regions that contains large contribution from Mn(II) were excluded from the rms calculation. These regions did not contribute to the minimization.

(48) Zheng, M.; Dismukes, G. C. *Inorg. Chem.* **1996**, *35*, 3307−3319.

(49) Diril, H.; Chang, H.-R.; Nilges, M. J.; Zhang, X.; Potenza, J. A.; Schugar, H. J.; Isied, S. S.; Hendrickson, D. N. *J. Am. Chem. Soc.* **1989**, *111*, 5102−5114.

(50) Geschwind, S.; Kisliuk, P.; Klein, M. P.; Remeika, J. P.; Wood, D. L. *Phys. Rev.* **1962**, *126*, 1684−1686.

(51) Barra, A. L.; Gatteschi, D.; Sessoli, R.; Abbati, G.-L.; Cornia, A. C.; Fabretti A.; Uytterhoeven, M. G. *Angew. Chem., Int. Ed. Engl.* **1997**, *36*, 2329−2331.

(52) We use the fact that the **g** tensor equations can be rigorously separated into two independent equations, one for the isotropic value and the other for the anisotropic component.

(53) de Wijn, H. W.; von Balderen, F. *J. Chem. Phys.* **1967**, *46*, 1381−1387.